An Ecological Land Cover Sampling Reclassification Model for Safety Estimation of Shoreline Systems from a Flood Defense Perspective Using Optical Satellite Remote Sensing Imaging

Dongju Wu * and Hui Xu

Water Conservancy and Hydropower Engineering, Hohai University, Nanjing 210098, China; hxu@hhu.edu.cn
* Correspondence: wudongju@hhu.edu.cn; Tel.: +86-25-8378-7325

Abstract: The safety level of a shoreline is essential for flood control projects and policy formulation or modification from both economic and environmental perspectives. With the development of remote sensing (RS) techniques, high spatial-spectral resolution and quick-revolution satellite images are now available and widely used in environment monitoring and management. It is therefore possible to more efficiently and conveniently identify the components of, and extract information for, shoreline environments. However, the problem is that the shoreline is always a long curve with a relatively narrow width, which limits the application of RS technology. This paper presents a method of recognizing different types of shoreline and of conveniently extracting the geographical coordinates of potential shoreline defense by analyzing and processing ecological information from an optical satellite RS data interpretation of land cover on both side of the shoreline. An application of this model in a low-resolution image case proved that the model can be used in the primary survey of a shoreline monitoring service platform as the basic tile level. The classification model is designed such that the requirements of image resolution for efficiently extracting information from the shoreline are low and the limitations imposed by a narrow shoreline width are avoided.

Keywords: land cover sampling; shore line identification; optical satellite RS data; edge feature enhancement; shoreline structure; ecological knowledge-oriented reclassification

1. Introduction

Along with the development of the economy and convenience of transportation, there is an increasing trend of people to migrate to shoreline areas, including coastal plains, deltas, and coastal areas [1], which are generally protected by flood defense structures, such as manmade dikes or gate-dams, natural embankments, dunes, and cliffs. In addition, economic activities are increasingly concentrated in shoreline areas [2]. As the industry develops and the economy booms in these areas, more land from river ways, lakes, or seas is occupied, which leaves less room for flood buffers. Although living with flooding has been proposed as an alternative to hazard control [3], the trend toward increased human activities in shoreline areas has not changed [4]. These activities are under pressure from streams constrained in riverbanks and sea water held back by sea dikes. Safety problems emerge at shorelines: flooding into these dynamic economic areas can lead to unbearable loss [5], as for instance the flooding of New Orleans in 2005. Considering the possibility of global climate change and extreme nature events, the shoreline areas will face real risks to society and the economy [3]. Fortunately, shoreline systems can also play a significant role in protection against water, flow diversion, irrigation, landscape, and traffic in these areas.

For these reasons, shoreline structures and their safety levels have become critically important and need more attention. This is urgent for both developed countries and developing countries.

In developed countries, although dikes and urban flood protection walls with channel improvement work have already been finished and work well in deltas or estuary zones, for instance, the Dike Ring and Delta Project in The Netherlands, external risk and some potential weak points and geotechnical structures still need monitoring and maintenance. In developing countries, the rapidly increasing development of booming cities and industrial areas near shorelines create a need for the design and construction on fragile natural levees, delta embankments, or sea beaches, and existing safety standards are often low. Because developed countries in many cases are ahead of developing countries, testing a proposed methodology in developed countries gives more insight and provides more experiences for reference. Hence, in this case study, a shoreline survey is applied in The Netherlands' coastal environment to explore the method of grasping the shoreline's safety level objectively, correctly, and integrally in real time, ideally for the RS monitoring system platform.

The current shoreline RS measurement and monitoring work with respect to flood defense, as an applied cross-disciplinary subject, is still at the primary stage, and mature shoreline structure applications of RS are basically in situ with preset sensors for Web service monitoring. De Vries et al. installed pore pressure sensors in a sea dike in Boston, UK [6]. Haarbrink and Shutko combined ground-measured data in Germany with data on airborne soil moisture to produce reliable brightness-temperature and soil-moisture maps [7] and tried to apply this method to dike safety detection based on temperature differences between the sea water and the dike's interior. Thiele et al. used a sensor-integrated geo-textile system to detect soil displacement in dikes [8]. Wang et al. developed a critical means of monitoring the snow cover increase and decrease process by using multiple temporal-coherence InSAR images [9]. Givehchi et al. applied remote data to seepage detection in dikes [10]. Meng and Wang indicated that high-resolution meteorological data for soil temperature and soil moisture is available for use in East Asia by developing a dataset model, called "CMADS" [11]. Hanssen et al. set metal plates on a dike and used radar interferometry information combined with LiDAR (Laser Imaging Detection and Ranging) data to calculate the displacement of the dike surface [12].

Ecological monitoring of shoreline areas with satellite imagery is mainly conducted on a large scale; for instance, sea level rise, coastal flood inundation, and the influence of human activities are detected using SAR imagery. Therefore, normal optical satellite data are rarely used for flood defense engineering, especially for investigations of the safety of shoreline structures. Because narrow shoreline widths require high-resolution data for interpretation, a great deal of system work is necessary to utilize RS observation. There are two direct ways to monitor the shoreline structure using RS technology: choosing an image with high resolution for monitoring important points or deploying sensors in the field. Both require knowledge of the key points or sections of a shoreline in advance.

In this paper, we explore an indirect method of knowledge-oriented analysis for monitoring shorelines with different scales of RS data. We combine commonly used optical satellite images from satellites such as Landsat and Sentinel-2 with shoreline environmental expert knowledge to make general judgments of the shoreline and identify potentially important points for further interpretation with high-resolution images or on-the-spot investigation. Based on this idea, this paper proposes a model that locates the shoreline first and then provides potential information on the type of shoreline structure and the weak points of detection by analyzing the land cover located near the shoreline in the satellite images.

The objectives of this paper are (1) to extract the geographic coordinates of the shoreline or potential shoreline defense; (2) to identify the ideal structure type for any point or section in the shoreline from the flood defense point of view; and (3), using ecological knowledge and RS image processing for further analysis and design, to produce a shoreline estimation model for deducing the type of safety structures that a given section of shoreline should have.

This paper contains three parts in terms of innovative content. First, the characteristics of the components and elements in a shoreline system needed for design and maintenance of shoreline defense are described and their spectral characteristics of surface feature are assessed.

Then, the edge enhancement method for extraction of line location for shoreline is presented. Finally, the reclassification model and procedure for shoreline identification and recognition of the type of shoreline defense structure are explained and illustrated.

2. Remote Sensing Data

2.1. Resolution Requirement for Linear Object

High-resolution RS imagery is widely used in various industries. When using them for land type classification, land cover is divided by its different reflection values or digital numbers in an RS grid image. A feature of the shoreline from the point of view of RS is its fine curve structure, and this is only for recognition and not sufficient for interpretation. Unlike normal large-scale applications of RS, such as agricultural and land use surveys, in a shoreline environment, knowing the relation between the spatial resolution of an RS image pixel and the spatial dimensions of the structure is necessary to recognize components and interpret shoreline information. Figure 1a,b show a pair of graphical raster images in the same amplification multiple on original images , with resolutions of 30 and 15 m, respectively, for a shoreline section on the east coast of the Dutch island of Texel, and where there is a dike for protection. The different clarity degree of the two images shows the impact of different raster resolutions on object recognition, although neither is adequate for recognizing the type of shoreline structure in detail. This is because the length of dike crests or other interesting features of a shoreline structure are generally no more than 3–5 m long, smaller than the resolution or pixel size of the images. In practice, we have found that an at least five- to eight-fold resolution is needed for observation.
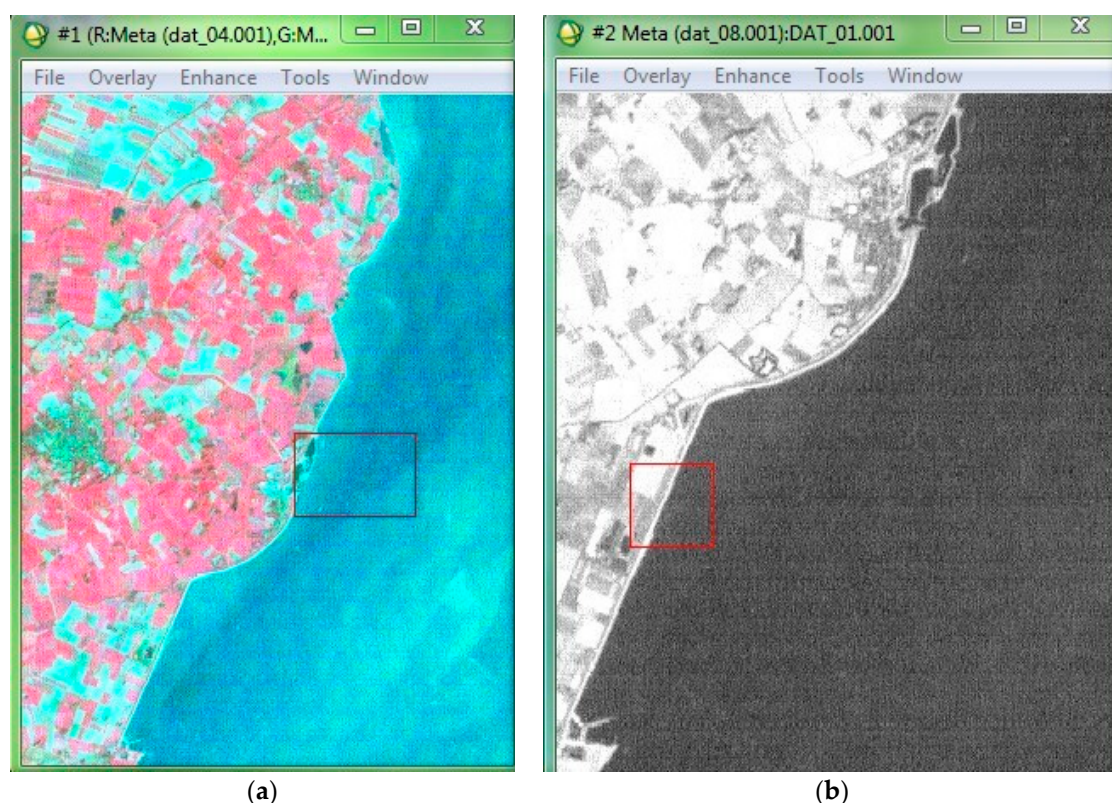

(**a**)　　　　　　　　　　　　　　　　　　　　(**b**)

Figure 1. (**a**) Raster image with a resolution of 30 m; (**b**) raster image with resolution of 15 m.

Therefore, when using RS imagery to detect and observe the shoreline with a long length but a narrow width, there is always a dilemma to face in terms of the scale size of the image resolution versus local the detailed information for the same study object. This paper tries to break this dilemma by

combining the satellite imagery with knowledge of flood defense and ecology to carry out information extraction work for shoreline structures.

2.2. Data and Case Study Area

The current study interprets an image acquired on 31 May 2001 from Landsat Enhanced Thematic Mapper Plus (ETM+), a passive optical image covering the north of The Netherlands. The data on that day provides far greater clarity than a cloudy day. In this season, the land has no snow cover; instead, vegetation and crops are in lush growth, which is useful for land cover recognition and classification. The shoreline areas in the north of The Netherlands, after developing for decades, have a typical coastal structure that is well designed and maintained with a perfect layout of land use and components of flood defense such as sea dikes, dunes, and hydraulic structures, which can be set as a standard for comparing with other cases.

2.3. Data Spectrum and Bands Choice

ETM+ provides eight spectral bands: six multispectral bands with a spatial resolution of 30 m, one panchromatic band with a resolution of 15 m, and one thermal infrared band with a spatial resolution of 60 m, respectively, covering the visible, near-infrared, and shortwave of the electromagnetic spectrum. The following are the spectral parameters and potential use of these different bands (Table 1).

Table 1. ETM+ bands and their main use.

Band Number	Band Scope	Wavelength (μm)	Resolution (m)	Use
1	Blue-green	0.45–0.515	30	Atmospheric qualities
2	Green	0.525–0.605	30	Green vegetation reflection
3	Red	0.63–0.69	30	Chlorophyll absorption band
4	NIR	0.75–0.90	30	Water/land interface contrast
5	SWIR	1.55–1.75	30	Moisture
6	TIR	10.4–12.5	60	Heat activities
7	SWIR	2.09–2.35	30	Rock and cloud properties
8	Pan	0.52–0.9	15	Geometrical characteristic

Different combinations of these bands are chosen for making different RGB model images to enhance the display of some ground objects on the screen or to improve the contrast between the study objects. The 4, 5, 3 band combination helps in identifying the water boundary because of its sensitivity to water content; however, it was discarded after our test since it classifies some wetlands or moist sands as water bodies, locating shorelines inland from the actual shoreline. In this study, the coastline needs to be picked out, so Band 4 is required, and sand vegetation and green crops need to be distinguished by the chlorophyll identification of plants using Band 3 and Band 2, so the combination of near-IR (Band 4), red (Band 3) and green (Band 2) is optimal. This 4, 3, 2 band combination is a standard false color composite; in this combination, the resulting image is similar to a colorized infrared image with defined water/land interfaces. Sand is presented as light blue. Vegetation displays are in several shades of red: bright red indicates the broad-leaved forest and healthy green plants, and pale red indicates sparse vegetation cover, scrubby plants, or jungles in sandy areas.

3. Shoreline System

3.1. Components of Shoreline System

As a part of an integrated flood defense, the shoreline system is a design and disaster management concept, and on the ground it is a conjunction of flood defense structures as well as an ecosystem that is probably affected by other human activities. In this paper, which aims to analyze the flood

defense structure types and risk levels of a section of shoreline, a "shoreline system" can be understood as a shoreline with its immediate and nearby land cover, or the position belt for a specific type of flood defense. That is, a shoreline system from the point of view of flood defense is comprised of three parts: firstly, the water body; secondly, the land cover and the areas of human activity near the shoreline; and thirdly, shoreline defense structures, including sea or river dikes, revetments, coastal beaches, flood walls, sand dunes, mounds, cliffs, buffer regions, secondary dry dikes, sluices, dams, and storm surge barriers. In this case study in the north of The Netherlands, three main components are considered in the shoreline: the dike, dunes, and the hydraulic structure.

A dike is generally considered to be an embankment for controlling the water in rivers or holding back seawater. In hydraulic engineering, it is either manmade or a strengthened embankment based on natural levees. Generally, it consists of one crest and two slopes along the water body on one side, but is more complicated when combined with other functions or structures. Figure 2a is a typical sea dike in Urk, The Netherlands.

A dune is a natural sea defense formed as wide sand hills but along the coastline. Dunes can have several peats and gulches, and can be desert, forest, or grass. Figure 2b shows a dune face near Noordwijk in The Netherlands.

Hydraulic structures in a shoreline system are mostly located in key positions to control water flow and obtain safety and convenience. Sluices, dams generally with a bridge surface, and storm surge barriers are common hydraulic structures in a shoreline system.

It is worth mentioning that, in dune shore sections, there are always narrow alluvial shores between the dune and sea; this association is common and appears frequently elsewhere; indeed, the North Sea takes sand to the west shore of The Netherlands. Dunes in Holland are accompanied by alluvial shores due to flushing of sea water in the last hydrology and climate period, not long ago. This kind of alluvial shoreline is part of the dune protection in Holland (except in the delta area, where such shores are protected by flood walls or hydraulic structure).

(**a**)	(**b**)

Figure 2. (**a**) A sea dike in Urk, The Netherlands; (**b**) A sand dune near Noordwijk, The Netherlands.

3.2. Characters of the Shoreline System

The safety of a shoreline system depends not only on shoreline structure but also on the requirements of human activities and environmental changes near the shoreline. Hence, we need to take into account features of not only the shoreline structure but also the shoreline environment. Shoreline characteristics generally include the following surfaces: water, soil, sand, forest, grass, metal structure, asphalt, and concrete.

Table 2 lists the characteristics and hydraulic parameters of dikes, dunes, and hydraulic structures from the point of view of RS and flood defense, along with the related RS methods.

Table 2. Characteristics of the components in shoreline system from the point of view of RS design.

Perspective	Dike	Dune	Hydraulic Structures
Spatial character	Lines; narrow width; along water body;	Along the coast with natural curve; hundred meters width with ups and downs; covered with bushes and grass;	Line or point; surrounded by water;
Structural character	Crest(s) and slopes, ditch;	Several peaks with trenches and cliffs;	Water level control; can be combined with traffic;
Material information	Clay; sand; rubble mound; concrete; revetment;	Sand; water; vegetation;	Steel; concrete;
Cover information	Sand; soil; concrete; grass; asphalt;	Sand plants; grass;	Concrete; asphalt; grass;
Hydraulic conditions	Water levels; surge; wind;	Storm surge level; sand transportation; dune foot line;	Water level difference;
Failure modes	Overflow; erosion; landslide; piping; seepage; moisture; liquefaction; cracks and caves; sinking;	Erosion; sliding;	Overflow; sliding; operability errors;
Changes in seasons	Vegetation; precipitation; water level;	Vegetation; surge level; sea wind;	Grass; asphalt and concrete aging;
Surface spectral character	Depending on concrete; asphalt; grass; sand; high resolution needed for mixed parts;	Raw texture; light red;	Concrete and steel;
RS method	Optical passive RS image for observation and identification from air; radar for surge; TIR image for seepage; InSAR for cliff/dune foot deformation detection or high surge level monitoring; LiDAR for elevation extraction; Sonar for structure underwater scanning.		

4. Shoreline Structure Estimation Model with Ecological Knowledge-Oriented Reclassification

4.1. Workflow of the Method

There are two essential elements for estimating the shoreline structure in this method as introduced in the first section: a reasonable shoreline location line and a logical land cover classification map. The main procedures for shoreline system estimation from a perspective of hydraulic engineering are illustrated in the following items, which are in line with the RS image preprocessing procedures, i.e., geometric transforming, spectrum transforming, and spatial subsets. Based on the band choice as mentioned previously, image fusion is processed to improve image resolution, and workflow goes in two parallel preparatory directions—one for water/land boundary delineation and shoreline extraction and another for an integrated ecological land cover map—until the shoreline structure is estimated according to the percentage calculation of the land cover in the buffer zone behind the shoreline. The workflow for the method of shoreline extraction, land cover classification, and shoreline structure estimation is represented in Figure 3.

The location of the shoreline can be extracted from the raster image, relying on its linear feature and position on the boundary of water and land. Accurately mapping of the shoreline is essential for laying out flood defenses and is needed later, in this case study, to calculate the percentage of the land cover around it.

RS classification identifies and recognizes different land cover pixels that are the same or similar to a group of the same category on the raster image by calculating radiation information from different land cover types. It does so according to the hypothesis that identical or similar earth covers dominate the pixels that are recording them, which is a valid assumption if the image resolution is quite high and can be matched to the density of the land cover. The classification method used in this study enabled us to recognize different farmlands, different dune areas, different sea water areas, and other landforms assembled on a large scale. We were therefore able to produce a corresponding preliminary classification map and extract locations, but we are unable to describe the shoreline structure in detail.
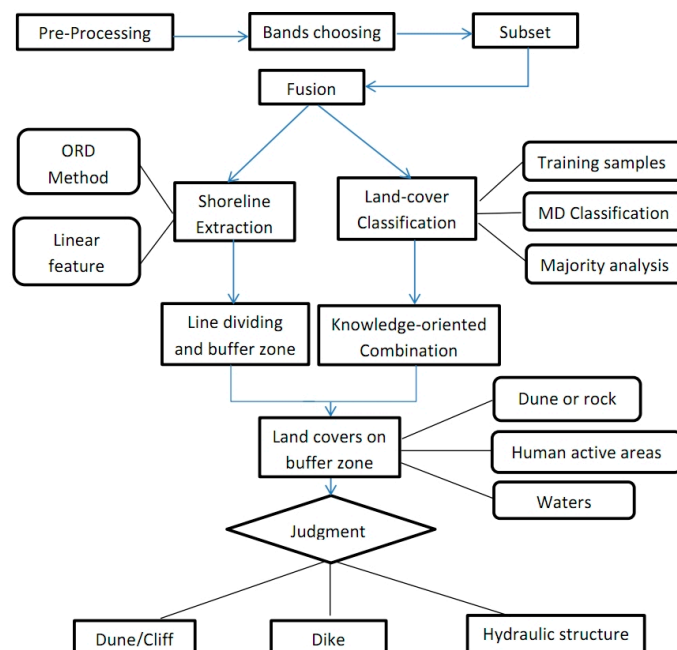
Figure 3. Ecological knowledge-oriented reclassification and estimation of shoreline structure.

Based on the information of the shoreline location and land cover information near the shoreline, by using ecological knowledge or other information such as altitude data, we were able to deduce shoreline structure types that constitute a flood defense and conform to the safety levels of a flood defense. The key of the estimation is the relationship between land cover information and the requirements of the flood defense. In the case study here, the sea dikes or flood walls are always built on the edge of the areas of human activity but without the protection of dunes or cliffs; hydraulic structures are always deployed at key positions of water flow and with linear features; dunes are usually along the shoreline and are several hundred meters in width. Therefore, recognition of areas of human activity is necessary and can be achieved by reclassifying residential areas, farmlands, and industrial areas as a group on the classification map. To recognize existing shoreline flood defense structure types or those that should be deployed along a section of shoreline, we propose a reclassification model based on categorizing the classification map such that the flood defense information related to the shoreline structure can be determined. The reclassification in this methodology is an artificial categorization of land cover for recognizing different levels of flood safety alone the shoreline. Other indexes or information extracted from other RS data or obtained from other sources—such as water level, quantity of flow, economic value behind the shoreline, and especially elevation extracted from LiDAR datasets—can be added to the corresponding image pixels for reclassification.

4.2. Shoreline Extraction

The shoreline in this study, used for sea defense, is located along the coastline and crosses the narrow part of the sea or estuary to form a flood defense safety system by controlling water levels while meeting Holland's requirements for transport and ecology. Because it is on the edge of the water or land, there is a clear line of demarcation on the special RS image (RGB Bands 4, 3 & 2) in Figure 4. Where the coastline largely consists of dunes, there can also be a light blue belt as a result of wet sands, and different waters such as sea water and lake water, have different colors that are recognizable both to the human eye and for computing values.

Extraction of the location of a shoreline is the precondition for accurate length and land cover calculation in estimation of shoreline structure later, and can benefit from image with a high resolution and a distinct boundary of water/land.
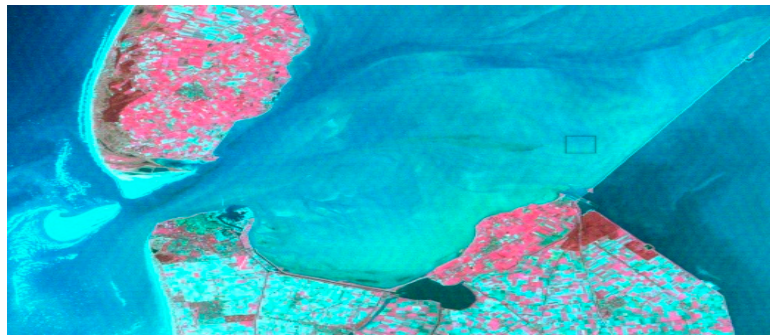
Figure 4. Line of demarcation in the shoreline system on ETM+ image with RGB Bands 4, 3 & 2.

4.2.1. Image Fusion

Image fusion is a grid image process that is done by resampling on a panchromatic (Pan) band image (seen in Figure 1b). Resampling is done at the maximum spatial resolution for bands from the same sensors and using a multispectral (MS) image with a low spatial resolution, to produce high-resolution multispectral data at the same spatial resolution as the panchromatic band [13,14]. Here, MS Bands 4, 3 & 2 and Pan from ETM+ data are chosen for image fusion using professional satellite image proceeding software ENVI by employing HSV (hue, saturation, and value color space) conversion [15,16]. Figure 5a,b respectively show the original and the fusion results at the same magnification scale, while Figure 6a,b show the high-resolution Google Satellite image of the same area and the detail of a port.
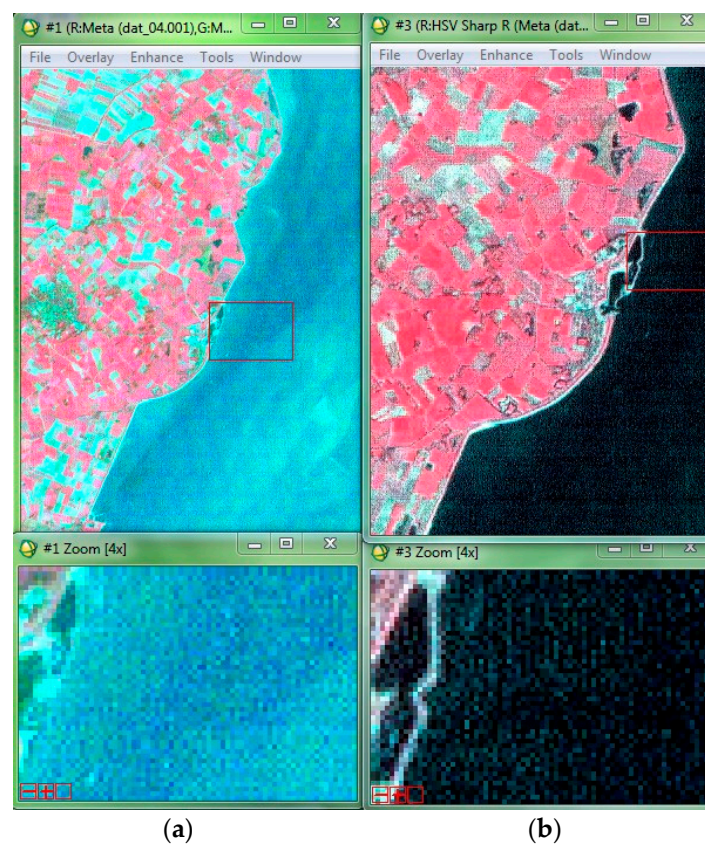

Figure 5. (**a**) Original image with a resolution of 30 m; (**b**) Fused image with a resolution of 15 m.

Figure 6. (**a**) High-resolution image of same area; (**b**) Detail of a port in the area.

4.2.2. Edge Feature Enhancement and Coastline Extraction

Based on the fused image, two filter operators of convolution, Roberts and Directional, are used to perform edge feature enhancement and obtain two separate images. Then, a false color RGB image is acquired by combining their first bands (the original sharpened image, Figure 7a; the Roberts image and the Directional image, ORD (original sharpening, Roberts and Directional filter operator enhancing) method, Figure 7b) to emphasize the coastline and remove the uncertainty of the boundary [17,18]. With clear boundaries and an obvious contrast between different objects, the location lines of the coastal shore can be calculated and extracted accurately by the tool Linear Feature Extraction with Intelligent Digitizer in ENVI and saved as a vector image file (seen in Figure 7c) [19].
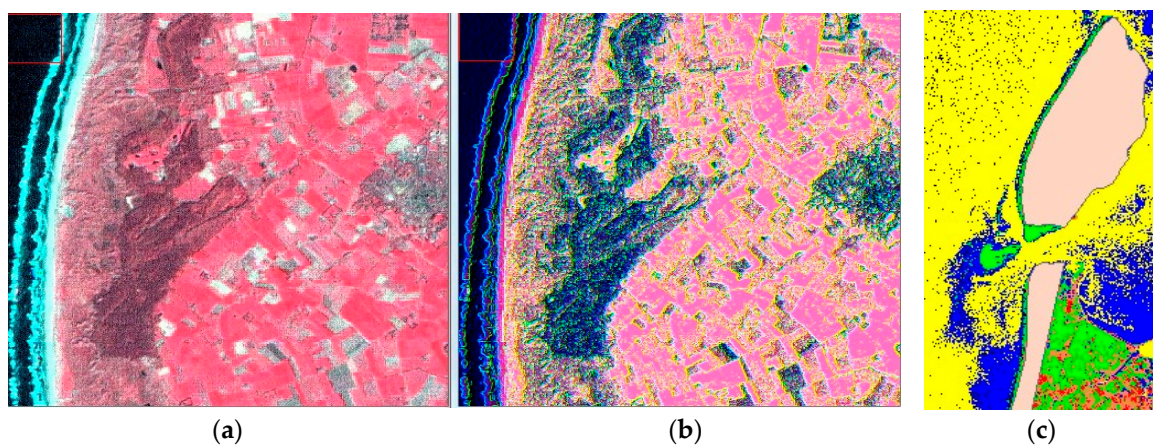

Figure 7. (**a**) Sharpened image; (**b**) ORD edge feature enhanced image; (**c**) Shoreline.

4.3. Classification and Reclassification

The process described immediately above was used to generate a land cover classification map and then integrate the dune areas and the areas of human activity by reclassification, in order to judge the type of the shoreline system segments in the next step. In short, classification was used to generate the land cover map, and reclassification was used for judgment of the shoreline structure.

4.3.1. Land Covers Classification

Training samples are finely set by ground objects with different spectral signatures even though they are the same thing in hydraulic engineering. In this case, four kinds of waters, four kinds of dune cover, crop land, bare land, and residential area were picked out and trained by setting a Region of Interest (ROI, seen in Table 3). Then, the supervised minimum distance classification method (result seen in Figure 8a) was applied to the fused image to create a basic land cover image shown in Figure 9a. By the process of majority analysis (result shown in Figure 8b), isolated pixels were transformed into the majority class surrounding them, and a smooth classification image was created. Results for comparison are shown in Figure 9b. The definition of isolation can be controlled by a threshold value.
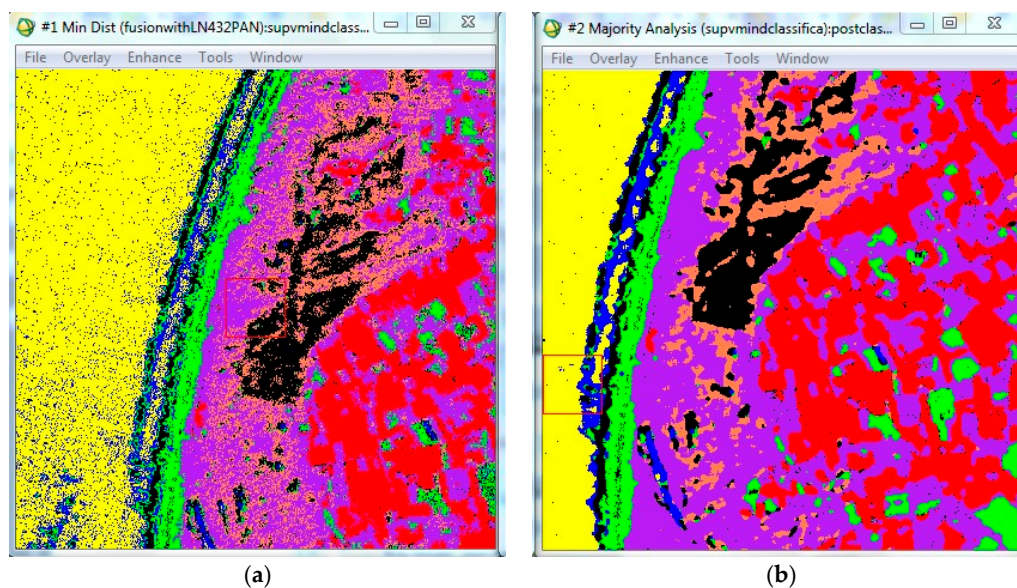

Figure 8. (**a**) Minimum distance classification; (**b**) Majority analysis for smoothing.
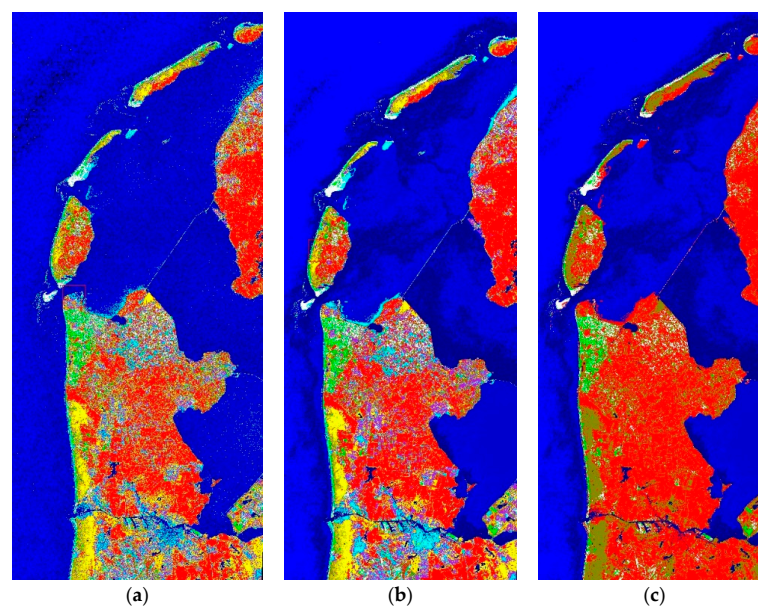

Figure 9. (**a**) Basic classification image; (**b**) Classification image after majority analysis processing; (**c**) Reclassification map after combination.
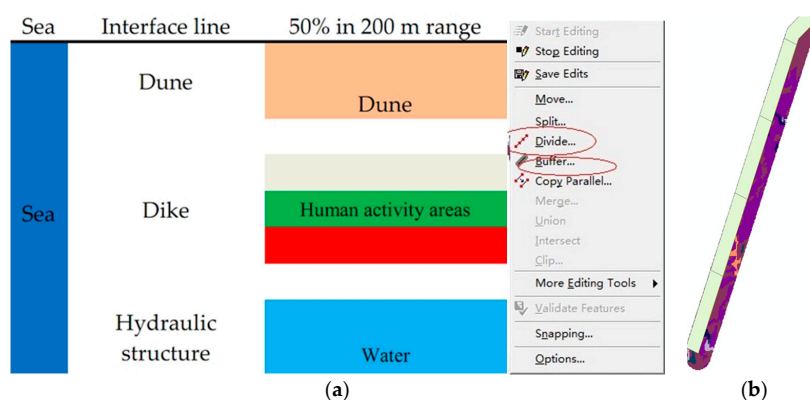
Table 3. Training sample list.

ROI Name	Color	Pixels	Polygons
Sea water	Blue	617,788	4/617,788
Offshore water	Blue 1	1,034,936	4/1,034,936
IJmeer water	Blue 2	607,603	3/607,603
Inland water	Blue 3	49,329	8/49,329
Dune dark red	Yellow	108,642	13/108,642
Dune light red	Yellow1	67,681	4/67,681
Dune grass	Yellow2	92,913	7/92,913
Dune land	Yellow3	61,601	8/61,601
Crop plant	Red	70,013	26/70,013
Sands	White	45,102	3/45,102
Town	Purple	198,240	16/198,240
Sand land	Green	13,984	9/13,984
Crop soil	Cyan	8615	8/8615

4.3.2. The Ecological Knowledge-Oriented Reclassification

In a map that classifies land cover, different classes may indicate that they have different spectral reflection; however, in another dimension, they may be in the same category: for instance, fields and towns can both be classified as areas of human activity. For logical analysis—for example, when the safety level of a section of shoreline based on to nearby land cover is to be determined—a reclassification in the land cover map is needed. In this study, all land cover related to dunes, including dune sands and dune plants, was turned into class D (in cyan) [20,21], and human-activity-related land cover [22], such as fields, towns, manufacturing, and other infrastructure lands are incorporated into class H (in red). The reclassification result is shown in Figure 9c. Colors are reset to contrast the differences in water bodies, dune areas, and areas of human activity in the images.

4.4. Estimation Principle for Shoreline Type

Dikes are (or should be) deployed on the edge of high-risk coast areas near human activity that lack the protection of dunes [23,24]; dunes are near the coastline and covered with sand or dune plants. The hydraulic structures either are located in a river mouth or delta area, or connect different lands. Therefore, based on a land-cover reclassification map and knowledge of the shoreline system structure in a certain area, an ecological knowledge-oriented method can be used to determine the safety level of a section of shoreline by calculating the percent of the D/H/water pixels behind the extracted shoreline in a certain range (here, 200 m). If the D pixels account for over 50%, then the corresponding coastline is dune coast; if the H pixels occupy more than 50%, then there is a need for dike defense; if water makes up the largest part, then a hydraulic structure is needed (seen in Figure 10a).

Figure 10. (**a**) Judgment of flood defense type for a shoreline system; (**b**) Buffer zone.

With the coastline's location information and the generated reclassification image, ArcGIS software was used to define a buffer zone, seen in Figure 10b, and extract the attributes for our shoreline classification judgments. Finally, a shoreline structure map was created, as shown in Figure 11.
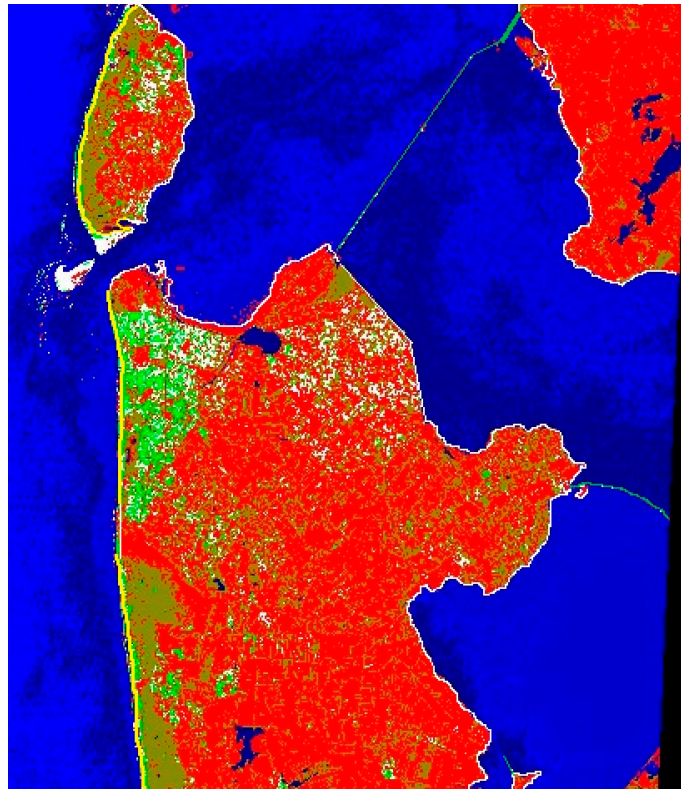

Figure 11. Shoreline structure map: dikes in white line, dunes in yellow line, and hydraulic structures in green line.

5. Result and Verification

The shoreline structure map seen in Figure 11 shows that the outer or western coastlines of The Netherlands are protected mostly by highly safe dune areas [25]. The inside, or IJmeer Lake side of the land–water boundaries are more protected by dikes, or need manmade flood defense [26]. The Afsluitdijk Dam and some wing dams can be recognized as hydraulic structures, seen in Figure 11.

5.1. Accuracy of Shoreline Extraction

To test the effect of our edge feature enhancement, shoreline extraction was performed three times for the coastline of the island of Texel, shown in Figure 11. This was performed separately, using image sharpening and edge-feature enhancement. Relative error was calculated with extracted data and measurements from Google Earth, using Equation (1).

$$\sigma = \frac{|L_e - L_m|}{L_m} \tag{1}$$

in which L_e is the extracted length; L_m is the measured length from Google Earth. The verification result is listed in Table 4.

Table 4. Result of extracted length verification.

No.	Length (m)			Relative Error σ (%)	
	L_m	L_e (Sharpened)	L_e (Edge Enhanced)	Sharpened Image	Edge Enhanced
1	59,300.64	55,252.379	57,008.213	6.82	3.87
2	59,300.64	56,828.006	57,015.823	4.17	3.85
3	59,300.64	56,766.758	57,056.754	4.27	3.78

The result shows that the filter operator of edge feature enhancement (ORD) largely reduces the error of length extraction compared to the sharpened image, which has the same high resolution of 15 m after the image fusion. This can be explained by the fact that the boundary of the water–land interface is becoming clear and a precise position of the shoreline can be located with less uncertainty via Fourier spatial transform and filtering noise [27]. This result also indicates that the geographic coordinates of the extracted line from the edge-enhanced image are closer to its real location than those of the boundary lines from the original or fused image.

5.2. Classification Accuracy

To evaluate classification effects, the overall accuracy and Kaapa coefficient of classification are listed in Table 5, which shows the two classifications' accuracy. "Overall accuracy" is the percentage of all pixels that were correctly classified; in this case, it also indexes the classification effect, since there are extensive pixels in each group of land cover is for comparison. The Kaapa coefficient shows the proportion of pixels that were wrongly classified pixels in comparison with the completely random classification.

The accuracy of both classifications is quite high, since land cover in the image of The Netherlands is very clear. The accuracy of our reclassification is higher than that of the major analysis classification, indicating that our reclassification logic is reasonable for land cover in a large group.

Table 5. Classification accuracy by confusion matrix results.

Classification	Overall Accuracy (%)	Kaapa Coefficient (%)
Classification after major analysis	84.2136	78.75
Reclassification	87.5932	83.92

5.3. Verification of Shoreline Structure Map

Based on tests with a field survey and a ground view of Google Earth, estimations of the shoreline structure can be considered realistic and reliable, even where different components of the shoreline meet. For example, a town with fields that are adjacent to the western coast of North Holland and that connect two dune areas along the coast is estimated as protected by a dike, which conforms to the actual situation, as seen in Figures 11 and 12a. It was determined that an island of human activity in the IJmeer Lake near the eastern end of the Afsluitdijk Dam should be protected by dikes or floodwalls, but that the shape of the island with its extensional stretches is unsuitable for building dikes; our test showed that there is a boat house area that needs to connect with outside water (seen in Figures 11 and 12b). Other interesting points or sections with unique phenomena on the shoreline were found: for example, ports are always in broken waterlines in areas of human activity and protected by wing dams. These exceptional areas can all be reasonably explained, and the model robustly predicted our verifications.

One misclassification for shoreline systems was found: a dike behind a dune was misclassified as a dune, as seen in Figure 13a. However, this problem is more one of shoreline extraction than one associated with our estimation method, because the newly developing dune in front of the dike is about 500 m wide but has a very low elevation, as seen in Figure 13b. This indicates that high-resolution

DEM datasets are needed in some sections to estimate shoreline type. Considering one study that showed that "GDEM is of little use in areas of low relief" [28], and GDEM'S elevation resolution of 20 m, LiDAR datasets with higher vertical resolution or other high-resolution DEM would be more helpful for shoreline system classification and estimation in terms of vertical direction in flat areas or low-land country, such as The Netherlands.

(**a**)   (**b**)

Figure 12. (**a**) Town adjacent to coast; (**b**) Boat house in an island.

(**a**)   (**b**)

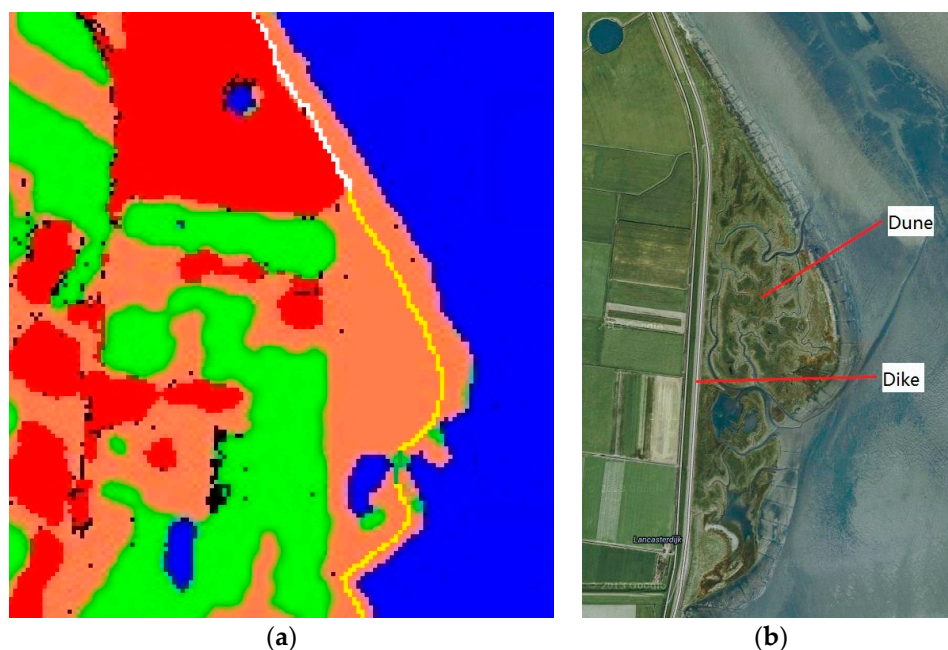**Figure 13.** (**a**) Misclassification of dike line; (**b**) A dike behind a developing dune.

6. Discussion and Conclusions

Some major points for further development and improvement of this model include the following:

1.   Appropriate spectrum analysis for both studied ground objects and band combinations from satellite or airborne sensors is needed for improving performance of the image and of object recognition when an optimal match is arranged.

2. Experience and knowledge about coastal areas is useful when boundary line extraction and shoreline extraction, for a particular purpose, is performed.

3. Some farmlands in The Netherlands consist of sandy soil and, in RS imagery, appear similar to sandy beaches. To distinguish them, further image processing, such as taking more training samples and overlaying different images with plants, is required.

4. The accuracy of this method can be verified in the field and largely depends on the accuracy of related knowledge and judgments, in addition to the processing skills required for an appropriate threshold value setting in classifying land cover.

The application of RS techniques is basically a scale problem from the data precision perspective. The ecological knowledge-oriented estimation method used in this study, since it is combined with a hydraulic safety requirement of the shoreline, is sensitive to the change in land cover along the shoreline and reliable after the test, despite the fact that the model is still a preliminary work for the application of RS to shoreline systems. With high-resolution images and the assistance of other information, this method should be able to give more useful indexes of shoreline sections.

Author Contributions: Dongju Wu and Hui Xu conceived and designed the experiments; Dongju Wu performed the experiments; Dongju Wu and Hui Xu analyzed the data; Dongju Wu wrote the paper.

Conflicts of Interest: The authors declare no conflict of interest.

References

1. Martínez, M.L.; Mendoza-González, G.; Silva-Casarín, R.; Mendoza-Baldwin, E. Land use changes and sea level rise may induce a "coastal squeeze" on the coasts of Veracruz, Mexico. *Glob. Environ. Chang.* **2014**, *29*, 180–188. [CrossRef]

2. Wang, M. The development trend and enlightenment of the advanced marine economy countries. *New Think.* **2012**, *3*, 40–45.

3. Klijn, F.; Van, B.M.; van Rooij, S.A. Flood-risk management strategies for an uncertain future: Living with Rhine river floods in The Netherlands? *Ambio* **2004**, *33*, 141–147. [CrossRef] [PubMed]

4. Holst, C.C.; Chan, J.; Tam, C.Y. Sensitivity of precipitation statistics to urban growth in a subtropical coastal megacity cluster. *J. Environ. Sci.* **2017**, *59*, 6–12. [CrossRef] [PubMed]

5. Burgess, K.; Townend, I. The impact of climate change upon coastal defence structures. In Proceedings of the 39th DEFRA Flood and Coastal Management Conference, York, UK, 29 June–1 July 2004.

6. De Vries, H.; Azzopardi, G.; Koelewijn, A.; Knobbe, A. Parametric Nonlinear Regression Models for Dike Monitoring Systems. In *Advances in Intelligent Data Analysis XIII, Proceedings of the 13th International Symposium, Leuven, Belgium, 31 October–1 November 2014*; Blockeel, H., van Leeuwen, M., Vinciotti, V., Eds.; Springer: London, UK; pp. 345–355, ISBN 978-3-319-12570-1.

7. Haarbrink, R.B.; Shutko, A.M. Simultaneous multi-sensor data for global information management system. In Proceedings of the Microwave Radiometry and Remote Sensing of the Environment, Firenze, Italy, 11–14 March 2008. [CrossRef]

8. Thiele, E.; Helbig, R.; Erth, H.; Krebber, K.; Nöther, N.; Wosniok, A. Dike monitoring. In Proceedings of the 14th International Symposium on Flood Defence: Managing Flood Risk, Reliability and Vulnerability, Toronto, ON, Canada, 6–8 May 2017.

9. Wang, Y.; Wang, L.; Li, H.; Yang, Y.Y.; Yang, T.L. Assessment of snow status changes using L-HH temporal-coherence components at Mt. Dagu, China. *Remote Sens.* **2015**, *7*, 11602–11620. [CrossRef]

10. Givehchi, M.; Vrijling, J.K.; Hartmann, A.; van Gelder, P.H.A.J.M.; van Baars, S. Application of remotely sensed data for detection of seepage in dikes. In Proceedings of the International Symposium on Resource and Environmental Monitoring, Hyderabad, India, 3–6 December 2002.

11. Meng, X.Y.; Wang, H. Significance of the China meteorological assimilation driving datasets for the SWAT Model (CMADS) of East Asia. *Water* **2017**, *9*, 765. [CrossRef]

12. Hanssen, R.F.; van Leijen, F.J. Monitoring water defense structures using radar interferometry. In Proceedings of the IEEE Radar Conference (RADAR), Rome, Italy, 26–30 May 2008. [CrossRef]

13. Goshtasby, A.A.; Nikolov, S. Image fusion: Advances in the state of the art. *Inf. Fusion* **2007**, *8*, 114–118. [CrossRef]

14. Gungor, O.; Boz, Y.; Gokalp, E.; Comert, C.; Akar, A. Fusion of low and high resolution satellite images to monitor changes on costal zones. *Sci. Res. Essays* **2010**, *5*, 654–662.

15. Li, S.; Yang, B.; Hu, J. Performance comparison of different multi-resolution transforms for image fusion. *Inf. Fusion* **2012**, *3*, 74–84. [CrossRef]

16. Zhang, Y. Understanding image fusion. *Photogramm. Eng. Remote Sens.* **2004**, *70*, 657–661.

17. Zhao, L.Y.; Ma, Q.L.; Li, X.R. Multi-spectral and panchromatic image fusion based on HIS-wavelet transform and MOPSO algorithm. *Acta Phys. Sin.* **2012**, *61*, 194204.

18. Li, Y.; Jin, W.; Yang, Y. HIS and DWT based remote sensing image fusion and its application on road extraction. In Proceedings of the International Conference on Consumer Electronics, Communications and Networks, Xianning, China, 16–18 April 2011; pp. 394–397.

19. Wang, N. Recognizing and extracting of roads in colourful map. *Comput. Eng. Des.* **2007**, *28*, 2642–2645.

20. Shi, C.H.; Wang, H. Forest canopy health classification of *Robinia pseudoacacia* planted based on linear spectral unmixing method and knowledge rules. *Geogr. Geo-Inf. Sci.* **2014**, *30*, 26–30.

21. Liu, Q.S.; Liu, G.H.; Yao, L. Detection of *Robinia Pseudoacacia* planted forest canopy health using landsat ETM image data. *Remote Sens. Technol. Appl.* **2008**, *23*, 142–146.

22. Mai, C.V.; Phajm, G.; Vrijling, J.K.; Mai, T.C. Risk analysis of coastal flood defenses—A Vietnam case. In Proceedings of the 4th International symposium on flood defence: Managing flood risk, reliability and vulnerability, Toronto, ON, Canada, 6–8 May 2008; pp. 931–938.

23. Jonkman, S.N.; van Gelder, P.H.A.J.M.; Vrijling, J.K. An overview of quantitative risk measures for loss of life and economic damage. *J. Hazard. Mater.* **2003**, *A99*, 1–30. [CrossRef]

24. Vrijling, J.K. Probabilistic design of water defence systems in The Netherlands. *Reliab. Eng. Syst. Saf.* **2001**, *74*, 337–344. [CrossRef]

25. Pilarczyk, K.W. Dutch experience on design of dikes and revetments. In *Coastal Engineering Practice*; Hughes, S.A., Ed.; American Society of Civil Engineers: New York, NY, USA, 2015; ISBN 978-0-87262-866-3.

26. Pilarczyk, K.W. Design of dikes and revetments—Dutch practice. In *Handbook of Coastal Engineering*; Herbich, J.B., Ed.; McGraw-Hill: New York, NY, USA, 2011; Chapter 3, ISBN 9780071344029.

27. Schowengerdt, R.A. Spatial transforms. In *Remote Sensing: Models and Methods for Image Processing*, 3rd ed.; Asbury, L., Lee, S., Washburn, B., Eds.; Academic Press: San Diego, CA, USA, 2006; pp. 229–284, ISBN 978-0-12-369407-2.

28. Hengl, T.; Reuter, H. How accurate and usable is GDEM? A statistical assessment of GDEM using LiDAR data. In Proceedings of the Geomorphometry, Redlands, CA, USA, 7–11 September 2011; pp. 45–48.